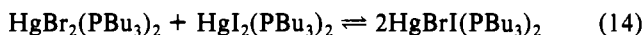


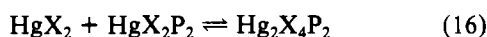
coupling constant consistent with the mixed-halide complex $\text{HgBrI}(\text{PBu}_3)_2$. It was deduced from these NMR experiments that the halide complexes undergo a typical Calingaert redistribution reaction.²⁴



Similar deductions are readily made from the electrochemical data (see eq 8). Halide-exchange reactions are observed to be extremely rapid from the NMR data which is consistent with all the electrochemical results which are characterized by reversible behavior and rapid exchange reactions involving X^- or HgX_2 . NMR and other studies on HgX_2 ²⁶ demonstrate the halide lability associated with these compounds. Mixtures of HgX_2 and HgX'_2 are known to be in equilibrium with their respective mixed species:

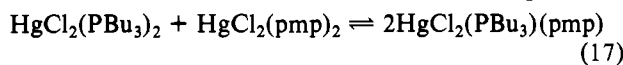


The same appears to be true of all related reactions such as



as required to interpret the electrochemical data.

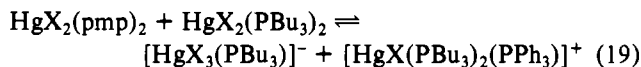
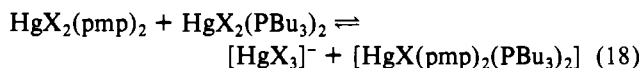
In NMR experiments,¹⁷ solutions of equimolar mixtures of $\text{HgCl}_2(\text{PBu}_3)_2$ and $\text{HgCl}_2(\text{pmp})_2$ at room temperature showed two ³¹P resonances with mercury satellites. The coupling constants were very similar to those of the starting materials although both resonances had moved toward each other. Two resonances in the mercury spectrum confirm that at room temperature there is no appreciable concentration of the mixed-ligand complex. At lower temperatures NMR resonances attributed to $\text{HgCl}_2(\text{PBu}_3)(\text{pmp})$ were reported. From electrochemical data, the redistribution reaction eq 17 in its



own right does not explain the exchange reaction occurring in this system. Our electrochemical results indicate that the mixtures containing different phosphine ligands require far more detailed investigation in order to provide a definitive account of the chemistry.

The available data are consistent with the fact that the mercury-halogen bond is weaker in the $\text{HgX}_2(\text{PBu}_3)_2$ com-

plexes than in the $\text{HgX}_2(\text{pmp})_2$ systems, while all the evidence suggests that the converse is true of the mercury-phosphorus bonds. Facile exchange reactions of the kind



in addition to other reactions would therefore be consistent with the electrochemical data at room temperature and partially account for the NMR data of the mixture not being exactly in agreement with the individually prepared solution with respect to the position of the HgX_2P_2 resonances. Presumably lower temperatures favor the reaction in eq 17 in preference to the reaction represented by eq 18 or 19. At this point in time it is clear that NMR data is inadequate for a complete understanding of the intricate range of equilibria and exchange reactions that can occur. Both electrochemical and NMR experiments indicate how facile the reactions between X^- , HgX_2 , HgX_2P_2 , $\text{Hg}_2\text{X}_4\text{P}_2$, etc. are. From the synthetic point of view, the system adjusts rapidly to its equilibrium position upon addition of any one of the compounds involved in the equilibrium.

In summary, the above examples demonstrate that under appropriate circumstances electrochemical techniques can provide a powerful approach to obtaining data of the kind widely obtained from NMR measurements. Work in these laboratories is continuing to develop a theory enabling a more quantitative approach to interpreting the data and to further investigation of the possible usefulness of the electrochemical approach.

Acknowledgment. The sabbatical leave of K. W. Hanck was supported by the Australian-American Educational Foundation (Fulbright Senior Scholar Award), by Deakin University (Gordon Fellowship), and by the National Science Foundation (Grant No. CHE78-24120). We gratefully acknowledge the contribution of the Australian Research Grants Committee in providing funds to support the experimental work.

Registry No. $\text{HgCl}_2(\text{PBu}_3)_2$, 41665-91-2; $\text{HgBr}_2(\text{PBu}_3)_2$, 20968-25-6; $\text{HgI}_2(\text{PBu}_3)_2$, 41665-93-4; $\text{HgCl}_2(\text{PPh}_3)_2$, 14494-85-0; $\text{HgBr}_2(\text{PPh}_3)_2$, 14586-76-6; $\text{HgI}_2(\text{PPh}_3)_2$, 14494-95-2; $\text{HgCl}_2(\text{pmp})_2$, 74039-80-8; $\text{HgBr}_2(\text{pmp})_2$, 75101-22-3; $\text{HgI}_2(\text{pmp})_2$, 75101-23-4; $(\text{C}_2\text{H}_5)_4\text{NCl}$, 56-34-8; $(\text{C}_4\text{H}_9)_4\text{NBr}$, 1643-19-2; $(\text{C}_4\text{H}_9)_4\text{NI}$, 311-28-4.

(25) J. C. Lockart, "Redistribution Reactions", Academic Press, New York, 1970.

(26) P. Peringer, *Inorg. Chim. Acta*, **39**, 67 (1980).

Contribution from the Chemistry Department, Nuclear Research Center "Demokritos", Aghia Paraskevi Attikis, Athens, Greece

Kinetics and Mechanism of the Reaction of Aqueous Europium(II) Ion with Pyruvic Acid

J. KONSTANTATOS,* E. VRACHNOU-ASTRA, N. KATSAROS, and D. KATAKIS

Received January 6, 1981

Eu^{II} ion reacts with pyruvic acid in air-free, aqueous, acidic solutions. The only organic product is lactic acid, which forms after a two-electron reduction of the keto form of pyruvic acid. The overall stoichiometry is 2:1, metal ion to organic acid, respectively. The kinetics were studied in detail by the stopped-flow technique. Under conditions of excess Eu^{II} ion over pyruvic acid, two stages are observed: a fast stage, which corresponds to the reduction of all available keto form in equilibrium with the hydro form of pyruvic acid, and a slow stage, during which hydrated pyruvic acid reacts only after being transformed to the carbonyl form by an acid-catalyzed reaction, which under these conditions is the rate-determining step. A mechanism is proposed and compared to the mechanisms of the corresponding reactions of the d elements Cr^{2+} , V^{2+} , and Ti^{3+} .

Introduction

In view of the biological importance of the hydrogenation of pyruvic and other keto acids, we decided to undertake an investigation of their redox behavior, using low-valent metal ions as probes. This is the third paper of the series and deals

with the reduction of pyruvic acid by the f-electron donor Eu^{2+} . The first two papers dealt with the reduction of pyruvic acid by the d-electron donors Cr^{2+} and V^{2+} ions. In using low-

(1) J. Konstantatos, N. Katsaros, E. Vrachnou-Astra, and D. Katakis, *J. Am. Chem. Soc.*, **100**, 3128 (1978).

valent metal ions, we take advantage of the following features.

(a) Relatively small differences in the reagents are "amplified" and may be reflected in completely different rate laws, stoichiometries, products, and mechanisms. Thus, reduction by Cr^{2+} , for example, proceeds by transfer to one molecule of pyruvic acid of two electrons from two metal ions, leading to the formation of a 2:1 chromium(III):lactate complex. In the reduction by V^{2+} the major product is dimethyltartaric acid.

In effect, by using different metal ions, one can focus on various aspects of the redox properties of pyruvic acid and hopefully single out those that are independent of the reducing agent.

(b) The low-valent metal ions react preferentially with the keto form of pyruvic acid. The hydro form is reduced only after being dehydrated. Moreover, the hydro to keto transformation serves as a convenient "internal clock" for the redox steps. Thus, in the system $\text{Cr}^{2+} + \text{pyr}^3$ this transformation is slow compared to the redox steps; in the system $\text{V}^{2+} + \text{pyr}$ it is fast. In the system $\text{Eu}^{2+} + \text{pyr}$ reported here the rates are comparable.

Experimental Section

Materials. Triply distilled water was used in all experiments. Solutions of Eu^{III} ion were prepared by dissolving europium(III) oxide in perchloric acid. Europium(II) perchlorate solutions were prepared from the above solutions by electrolytic reduction as described previously.⁴ They were kept under argon atmosphere to avoid air oxidation and in the dark to prevent photochemical oxidation.⁵ The concentration of europium(II) and europium(III) ions was checked spectrophotometrically, on a Cary 14 spectrophotometer, or amperometrically, on a Metrohm A.G. Herisau potentiograph, No. 436. Dimer-free pyruvate was supplied by Fluka and stored in a refrigerator. Stock solutions were prepared the day of their use, because pyruvic acid slowly dimerizes.

Reclaiming of Europium. Europium(III) was recovered from reacted solutions by precipitating as europium(III) oxalate. The precipitate was then filtered, washed, dried, and finally decomposed to europium(III) oxide in an oven at 900 °C. The oxide was analytically pure, and it was used to prepare new solutions.

Stoichiometry. The stoichiometry of the overall reaction was determined both in presence of excess Eu^{II} ion over pyruvic acid and vice versa. In the first case, the unreacted Eu^{II} ion concentration was determined by adding an aliquot of a deaerated Fe^{III} solution in aqueous sulfuric acid and titrating the resulting Fe^{II} with standard Ce^{IV} solution amperometrically on the potentiograph. In the second case, Eu^{III} ion was precipitated as oxalate. After filtration, the unreacted pyruvic acid, in the filtrate, was determined polarographically, in a citrate-phosphate buffer at pH 3.95, with use of a Metrohm A.G. Herisau rapid polarograph. The excess of oxalic acid did not affect the polarographic wave of pyruvic acid.

Reaction Products. The organic product of the reaction was isolated from the reaction mixtures by extraction with ether. Its identification was done by elemental analysis and mass spectrometry and from its NMR spectrum.

Kinetic Measurements. The kinetics were followed spectrophotometrically with use of an Applied Photophysics stopped-flow apparatus. The working wavelength for all runs was 402 nm. At this wavelength aqueous europium(II) ion has an absorptivity $\epsilon = 24$ whereas europium(III) ion is practically transparent.

For cases of large concentrations of the absorbing species, Eu^{II} , for which transmittance values were of the order of ~5% a 10- to 20-fold increase in the sensitivity of the stopped-flow instrument was

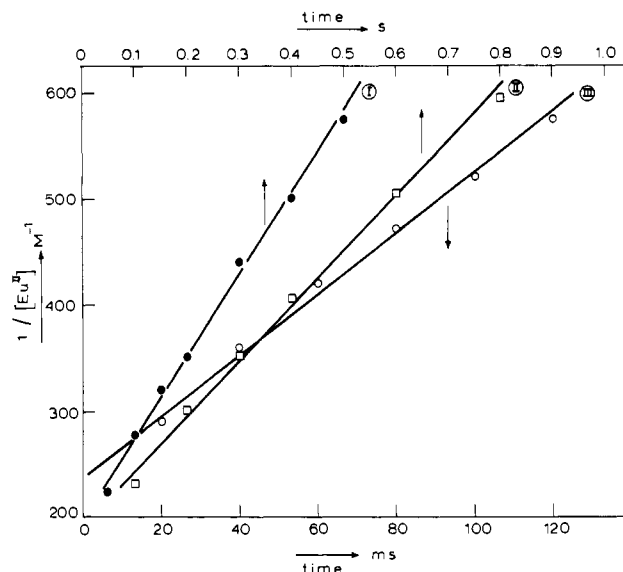


Figure 1. Typical pseudo-second-order plots for the reaction between Eu^{II} ion and pyr ($[\text{Eu}^{\text{III}}]$, $[\text{pyr}]$, and $[\text{H}^+]_0$ in large excess over $[\text{Eu}^{\text{II}}]_0$). I: $[\text{Eu}^{\text{II}}]_0 = 5.8 \times 10^{-3}$ M, $[\text{Eu}^{\text{III}}]_0 = 0.100$ M, $[\text{pyr}]_0 = 0.100$ M, $[\text{H}^+]_0 = 0.45$ M. II: $[\text{Eu}^{\text{II}}]_0 = 5.8 \times 10^{-3}$ M, $[\text{Eu}^{\text{III}}]_0 = 0.030$ M, $[\text{pyr}]_0 = 0.100$ M, $[\text{H}^+]_0 = 0.50$ M. III: $[\text{Eu}^{\text{II}}]_0 = 5.8 \times 10^{-3}$ M, $[\text{Eu}^{\text{III}}]_0 = 0.150$ M, $[\text{pyr}]_0 = 0.100$ M, $[\text{H}^+]_0 = 0.45$ M.

adequate in order to obtain good measurements. Although values for the transmittance at "infinite" time could not be determined very accurately under these conditions, this did not affect the values of the rate constant, since all these cases correspond to pseudo-first-order kinetics.

The range of values for the initial concentrations of Eu^{II} ion is not too extensive (2.5×10^{-2} – 5.0×10^{-3} M) because of the instrumental limitations and the inherent characteristics of the reaction. The rate law is nevertheless cross-checked under a variety of experimental conditions (see Results).

Results

Products and Stoichiometry. In strongly acidic solutions, the only organic product identified was lactic acid. The overall stoichiometry of the reaction was always found to be one organic molecule to two metal ions, irrespective of the initial concentrations of the reacting solutions.

Spectra. The absorption spectra of Eu^{II} and Eu^{III} species were taken on the Cary 14, and they agreed with those reported in the literature.⁴

Kinetics. (a) The rate of the reaction of aqueous Eu^{II} ion with pyr was followed for concentrations of pyr and hydrogen ion in excess over Eu^{II} ion. Under these conditions the order with respect to Eu^{II} is not simple; it changes between the values of 1 at the start to the value 2 at the end of the reaction.

(b) Previous experience⁴ suggested that this change in the order could be attributed to retardation by Eu^{III} , the concentration of which is building up during the reaction. The role of Eu^{III} ion was investigated by adding it in large excess over Eu^{II} . The excellent transparency of Eu^{III} at the working wavelength (402 nm) excluded technical complications. Under these new conditions, kinetics were simplified and the rate of the reaction was found to be second order with respect to Eu^{II} . Typical pseudo-second-order plots are shown in Figure 1. The corresponding kinetic data are given in Table Ia. Table Ia contains kinetic data obtained under different initial concentrations of hydrogen ion and pyr. These data clearly show that the rate of the reaction is indeed inversely proportional to Eu^{III} ion concentration and that $k^2(\text{obsd})$ is also directly proportional to pyr and hydrogen ion concentration. $k^2(\text{obsd})$ therefore, certainly encompasses the terms $[\text{H}^+]$, $[\text{pyr}]$, and $[\text{Eu}^{\text{III}}]^{-1}$.

(c) The reaction was further investigated with Eu^{II} ion and hydrogen ion in excess over pyr. The reaction then occurs in

- (2) J. Konstantatos, E. Vrachnou-Astra, N. Katsaros, and D. Katakis, *J. Am. Chem. Soc.*, **102**, 3035 (1980).
- (3) In this paper pyruvic acid is abbreviated by pyr, and its hydrated and keto forms are abbreviated by pyr(hydro) and pyr(keto), respectively.
- (4) (a) H. Taube and H. Myers, *J. Am. Chem. Soc.*, **76**, 2103 (1954); (b) S. Isied and H. Taube, *ibid.*, **95**, 8198 (1973); (c) A. Haim, *Acc. Chem. Res.*, **8** (1975); (d) E. Vrachnou-Astra and D. Katakis, *J. Am. Chem. Soc.*, **97**, 5357 (1975).
- (5) D. L. Douglas and D. M. Yost, *J. Chem. Phys.*, **17**, 1345 (1949).

Table I. Kinetic Data for the Reduction of pyr by Eu^{II} Ion at 25 °C

a. [Eu ^{III}] ₀ , [pyr] ₀ , [H ⁺] ≫ [Eu ^{II}] ₀						
[Eu ^{II}] ₀ 10 ³ , M	[Eu ^{III}], M	[pyr], M	[H ⁺], M	k ² (obsd)	2k ₁ k ₂ /k ₋₁ ^a	
5.8	0.100	0.100	0.50	830 ± 30	4150	
5.8	0.100	0.100	0.45	750 ± 25	4167	
5.8	0.050	0.100	0.45	1420 ± 60	3950	
5.8	0.030	0.100	0.50	2750 ± 110	4125	
5.8	0.150	0.100	0.45	490 ± 20	4083	
5.8	0.200	0.100	0.50	390 ± 15	3900	
5.8	0.100	0.200	0.50	1570 ± 50	3925	
5.8	0.100	0.250	0.50	2050 ± 85	4100	
5.8	0.100	0.150	0.50	1225 ± 40	4083	
5.8	0.100	0.100	0.90	1410 ± 75	3917	
5.8	0.100	0.100	0.35	575 ± 25	4107	
5.8	0.100	0.100	0.75	1270 ± 50	4233	
5.8	0.100	0.100	1.40	2165 ± 75	3866	
b. [Eu ^{III}] ₀ = 0; [Eu ^{II}] ₀ , [H ⁺] ≫ [pyr]						
[Eu ^{II}] ₀ , M	[pyr], M	[H ⁺], M	k ⁱ (obsd)/2 ^b	k ⁱⁱ (obsd)/2 ^b	k ⁱ (obsd)/2[H ⁺]	k ⁱⁱ (obsd)/[H ⁺][Eu ^{II}]
0.0125	0.0025	0.25	0.79	14.05	3.16	4496
0.0250	0.0025	0.25	0.80	29.14	3.20	4661
0.0240	0.0020	0.50	1.54	55.50	3.08	4625
0.0060	0.0005	0.40	1.29	10.90	3.23	4558
0.0100	0.0025	2.00	5.98	~90 ^c	2.99	~4500
0.0100	0.0025	0.25	0.82	11.4	3.28	4560
0.0200	0.0025	1.00	3.10	~90 ^c	3.10	~4500
0.0093	0.0012	1.00	2.95	42.0	2.95	4519
0.0109	0.0010	1.00	2.94	48.0	2.94	4406
c. [Eu ^{III}] ≫ [Eu ^{II}] ≫ [pyr(keto)]						
[Eu ^{III}], M	[Eu ^{II}], M	[pyr], M	[H ⁺], M	k ⁱⁱⁱ (obsd)		
				exptl	calcd	
0.180	0.005	0.0005	0.50	0.280	0.270	
0.500	0.005	0.0020	0.50	0.104	0.100	
0.180	0.005	0.0010	1.00	0.520	0.540	
0.500	0.005	0.0005	1.00	0.195	0.200	

^a The calculation was done with use of [pyr(keto)] = 0.42 [pyr] and k₁k₂/k₋₁ = 2025 ± 85 L mol⁻¹ s⁻¹. The uncertainties were calculated by least squares. ^b kⁱ(obsd) and kⁱⁱ(obsd) refer to the slow and fast stages of the reaction, respectively. ^c Values are approximate since they were at the limit of the stopped-flow instrument. k₁ = 2280 ± 80, k₂/k₋₁ = 0.90, and k₄ = 3.10 L mol⁻¹ s⁻¹. The uncertainties were calculated by least squares.

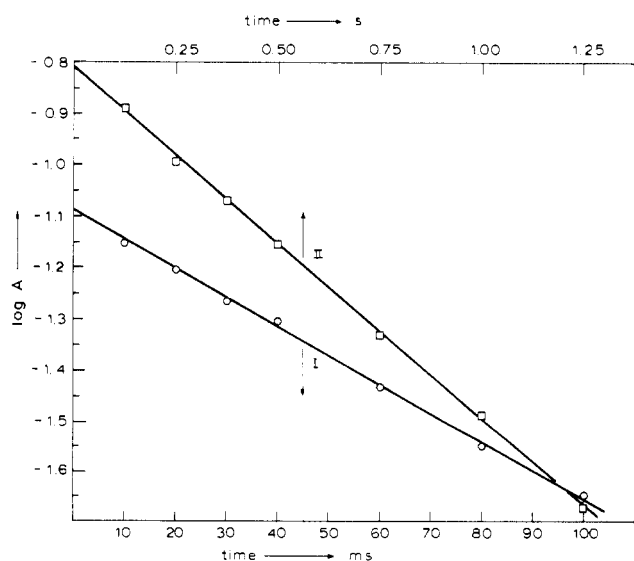


Figure 2. Typical pseudo-first-order plots for the reaction between Eu^{II} ion and pyr at 25 °C under conditions of [Eu^{III}]₀ = 0 and [Eu^{II}]₀, [H⁺]₀ ≫ [pyr]₀. Straight lines I and II correspond to the time resolved for the fast and slow stages, respectively. [Eu^{II}]₀ = 0.0125 M, [HClO₄]₀ = 0.25 M, and [pyr]₀ = 0.0025 M. A is the absorbance.

two stages. Both of these stages follow first-order kinetics with respect to pyr and hydrogen ion, but whereas the rate of the fast stage is also first order with respect to Eu^{II} ion concen-

Table II. Kinetic Data for the Reduction of pyr by Eu^{II} Ion at 25 °C; [pyr]₀ ≫ [Eu^{II}]₀, [Eu^{III}]₀ = 0

[Eu ^{II}] ₀ , M	[pyr] ₀ , M	[H ⁺], M	S(exptl)	S(calcd) ^a
0.006	0.100	0.50	78	85
0.006	0.150	0.25	62	63.8
0.004	0.150	0.20	48	51.0
0.004	0.100	0.20	33	34.0

^a S(calcd) = 2k₁k₂/k₋₁[H⁺][pyr(keto)], where [pyr(keto)] = 0.42[pyr].

tration, the rate of the slow stage is zero in this reactant. Typical pseudo-first-order plots are shown in Figure 2. Kinetic data derived under the conditions of the present section are reported in Table II. The presence of Eu^{III} ion in small amounts did not affect these kinetic data. If the amount of Eu^{III} ion, however, becomes comparable to that of Eu^{II}, the time scales of the two stages of the reaction become comparable, too. The observed rate constant, k(obsd), for the slow step is acid dependent and agrees well^{1,6,7} with that for the pyr(hydro) to pyr(keto) transformation. In addition, the decrease in absorbance at the end of the fast stage is 45 ± 5%

- (6) (a) D. E. Tallman and D. L. Leussing, *J. Am. Chem. Soc.*, **91**, 6253, 6256 (1969); (b) M. Becker, *Ber. Bunsenges. Phys. Chem.*, **68**, 669 (1964); (c) H. Strehlow, *ibid.*, **66**, 392 (1963).
 (7) (a) Y. Pocker, J. E. Meany, B. J. Nist, and C. Zadorojny, *J. Phys. Chem.*, **73**, 2879 (1969); (b) Y. Pocker, J. E. Meany, and C. Zadorojny, *ibid.*, **75**, 792 (1971).

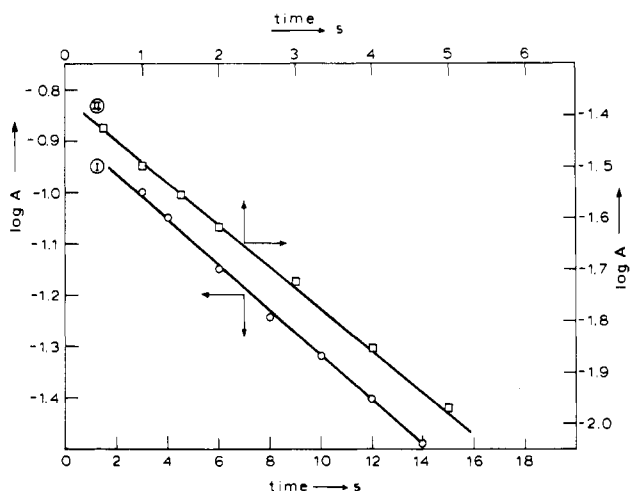
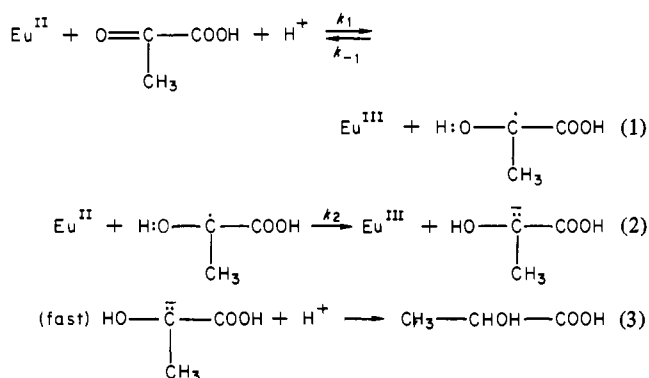


Figure 3. Pseudo-first-order plots for the reaction between Eu^{II} ion and pyr ($[\text{Eu}^{\text{III}}]_0 \gg [\text{Eu}^{\text{II}}]_0 \gg [\text{pyr}]_0$). I: $[\text{Eu}^{\text{III}}]_0 = 0.180 \text{ M}$, $[\text{Eu}^{\text{II}}]_0 = 0.005 \text{ M}$, $[\text{pyr}]_0 = 0.0005 \text{ M}$, $[\text{HClO}_4]_0 = 0.50 \text{ M}$. II: $[\text{Eu}^{\text{III}}]_0 = 0.500 \text{ M}$, $[\text{Eu}^{\text{II}}]_0 = 0.005 \text{ M}$, $[\text{pyr}]_0 = 0.0010 \text{ M}$, $[\text{HClO}_4]_0 = 0.50 \text{ M}$. A is the absorbance.

Scheme I



of the total decrease. This value was calculated by extrapolating kinetic curves such as those of Figure 2, and it agrees with the percentage^{1,6,7} of the keto form of pyr in equilibrium with the hydro form.

(d) When Eu^{II} ion concentration was in large excess over the concentration of pyr and Eu^{III} ion was present in large excess over Eu^{II} ion, first-order kinetics were observed. The kinetic data are reported in Table Ic. The pseudo-first-order rate constant, $k^{\text{iii}}(\text{obsd})$, is proportional to hydrogen ion concentration. It is also clear from these runs that $k^{\text{iii}}(\text{obsd})$ is inversely proportional to the concentration of Eu^{III} ion. Pseudo-first-order rate plots for two different concentrations of Eu^{III} ion are given in Figure 3.

Discussion

After considering the kinetic data reported in the results, we propose the reaction series given in Scheme I.

Reaction 1 may be preceded by a fast complex formation preequilibrium. Inhibition by Eu^{III} ion is tentatively attributed to the reaction of this ion with the intermediate free radical. If we assume reaction 3 to be fast and free radical, H:O- $\dot{\text{C}}$ (CH₃)-COOH, concentration to be steady, the following rate equation is derived:

$$-\frac{1}{2} \frac{d[\text{Eu}^{\text{II}}]}{dt} = \frac{d[\text{lactic}]}{dt} = \frac{k_1 k_2 [\text{Eu}^{\text{II}}]^2 [\text{H}^+] [\text{pyr}(\text{keto})]}{k_{-1} [\text{Eu}^{\text{III}}] + k_2 [\text{Eu}^{\text{II}}]} \quad (\text{I})$$

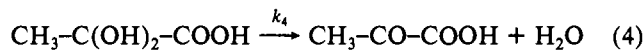
According to (I), as Eu^{II} ion concentration declines and Eu^{III} ion concentration builds up, the order with respect to Eu^{II} ion

should change from 1 to 2 under conditions of excess pyr(keto) and H⁺ (see Results, section a). When $k_{-1}[\text{Eu}^{\text{III}}] \gg k_2[\text{Eu}^{\text{II}}]$, eq I simplifies to

$$-\frac{d[\text{Eu}^{\text{II}}]}{dt} = \frac{2k_1 k_2 [\text{Eu}^{\text{II}}]^2 [\text{H}^+] [\text{pyr}(\text{keto})]}{k_{-1} [\text{Eu}^{\text{III}}]} \quad (\text{II})$$

and $k^2(\text{obsd})$ can be identified with $2k_1 k_2 / k_{-1} ([\text{H}^+] [\text{pyr}(\text{keto})] / [\text{Eu}^{\text{III}}])$. The data in Table Ia give the value for the composite constant $k_1 k_2 / k_{-1} = 2025 \pm 85 \text{ L mol}^{-1} \text{ s}^{-1}$.

The slower of the two stages observed under the conditions stated in the Results, section c, is interpreted if the reaction



is included in the mechanism. During the fast stage Eu^{II} ion reduces the equilibrium quantity of the keto form of pyruvic acid, which is 42% of the total pyruvic acid. Kinetics for this part of the reduction are described by rate equation I, which for $[\text{Eu}^{\text{II}}] \gg [\text{pyr}(\text{keto})]$ is approximated to

$$-\frac{d[\text{Eu}^{\text{II}}]}{dt} = 2k_1 [\text{Eu}^{\text{II}}] [\text{H}^+] [\text{pyr}(\text{keto})] \quad (\text{III})$$

Kinetic data in Table Ib fit eq III, $2k_1 [\text{Eu}^{\text{II}}] [\text{H}^+]$ can be identified with $k^{\text{ii}}(\text{obsd})$, and we obtain $k_1 = 2280 \pm 80 \text{ L mol}^{-1} \text{ s}^{-1}$. The ratio k_2 / k_{-1} can also be calculated now: $k_2 / k_{-1} = 0.90$. Kinetics of the slow stage are even simpler as they can be assigned to reaction 4, which under these conditions becomes the rate-determining step.

If we assume steady state for the keto form we obtain

$$-\frac{d[\text{Eu}^{\text{II}}]}{dt} = 2k_4 [\text{pyr}(\text{keto})] \quad (\text{IV})$$

The data in Table Ib give a value $k_4 = k^{\text{i}}(\text{obsd})/2 = 3.10 \text{ L mol}^{-1} \text{ s}^{-1}$, which is in excellent agreement with the value 3.20 reported by the authors¹ in a previous work.

Under conditions such as $[\text{Eu}^{\text{III}}] \gg [\text{Eu}^{\text{II}}] \gg [\text{pyr}]$ and rather low absolute concentration of Eu^{II} ion (Results, section d; Table Ic), the observed rate constant agrees nicely with that calculated on the basis of the rate equation (I), where $[\text{pyr}(\text{keto})]$ should now be replaced by $[\text{pyr}]$.

With hydrogen ion and pyr(keto) in large excess over Eu^{II} ion integration of eq I gives

$$\frac{x_0}{x} - \left(\frac{k_2}{k_{-1}} - 1 \right) \ln x = S t + \frac{x_0}{x_0 - x_3} - \left(\frac{k_2}{k_{-1}} - 1 \right) \ln (x_0 - x_3) \quad (\text{V})$$

$$x_0 = [\text{Eu}^{\text{II}}]_0 + [\text{Eu}^{\text{III}}]_0 \quad x = [\text{Eu}^{\text{II}}]_t$$

$$x_3 = [\text{Eu}^{\text{III}}]_0 \quad S = k_1 k_2 / k_{-1} [\text{pyr}(\text{keto})] [\text{H}^+] \quad (\text{VI})$$

Plots of the data in section a of the Results based on eq V are given in Figure 4. From these plots, for which $x_3 = [\text{Eu}^{\text{III}}]_0 = 0$ and $x_0 = [\text{Eu}^{\text{II}}]_0$, we obtain S . This parameter is also calculated with use of eq VI, and the independently determined values of the rate constants, calculated and experimental, are in very good agreement.

When Eu^{III} ion is present and is in large excess over the Eu^{II} ion ($x_0 \approx [\text{Eu}^{\text{III}}]_0$ and $x_0/x \gg (k_2/k_{-1} - 1) \ln x$), eq V is approximated to

$$1/x = S/[\text{Eu}^{\text{III}}]_0 t + 1/x_{\text{initial}}$$

This last equation is the integrated second-order equation applied in section b of the Results to derive the data reported in Table Ia. $k^2(\text{obsd})$ is therefore identified with $S/[\text{Eu}^{\text{III}}]_0$.

It was mentioned in the Introduction that the hydro to keto transformation serves as a convenient "internal clock". In the

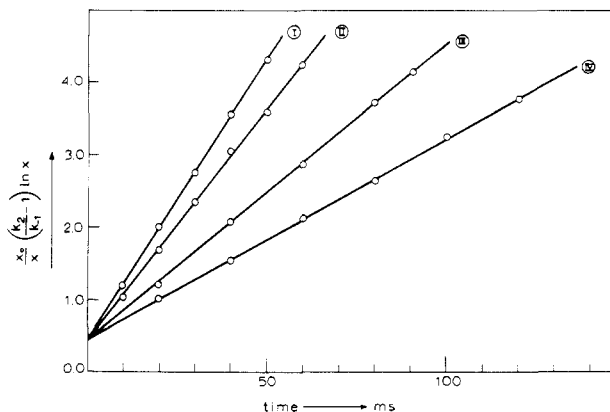
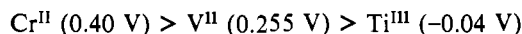


Figure 4. Plots of the equation $x_0/x - (k_2/k_{-1} - 1) \ln x = St + 1 - (k_2/k_{-1} - 1) \ln x_0$. All runs were 0.005 M in $[\text{Eu}^{\text{II}}]_0$. I: $[\text{Eu}^{\text{III}}]_0 = 0.180 \text{ M}$, $[\text{pyr}]_0 = 0.0005 \text{ M}$, $[\text{H}^+]_0 = 0.50 \text{ M}$. II: $[\text{Eu}^{\text{III}}]_0 = 0.500 \text{ M}$, $[\text{pyr}]_0 = 0.0020 \text{ M}$, $[\text{H}^+]_0 = 0.50 \text{ M}$. III: $[\text{Eu}^{\text{III}}]_0 = 0.180 \text{ M}$, $[\text{pyr}]_0 = 0.0010 \text{ M}$, $[\text{H}^+]_0 = 1.00 \text{ M}$. IV: $[\text{Eu}^{\text{III}}]_0 = 0.500 \text{ M}$, $[\text{pyr}]_0 = 0.0005 \text{ M}$, $[\text{H}^+]_0 = 1.00 \text{ M}$.

reaction between Cr^{II} ion and pyruvic acid¹ this transformation is rate determining. In the reaction between V^{II} ion and pyruvic acid² the redox reaction is rate determining. The corresponding overall redox reaction of Ti^{III} ion is even slower.⁸

The rates of these d ions correlate with their oxidation potentials:



On this scale f-donor Eu^{II} ion with an oxidation potential of 0.43 V is expected to react slightly faster than Cr^{II} ion. It does not. The explanation should not perhaps be sought in the redox reaction per se, but in the preceding complex formation (preequilibria, not depicted in the mechanism). It is reasonable to expect that complex formation via the d orbitals of Cr^{II} is more effective than formation via the f orbitals of Eu^{II} ion.

In the reaction of pyruvic acid with V^{II} ion the rate, in the range 0.5–2.5 M HClO_4 , is independent of hydrogen ion concentration. In the corresponding reaction of Eu^{II} ion a linear dependence on hydrogen ion concentration is observed. It can be argued that in both cases the rate-determining electron-transfer step is catalyzed by hydrogen ion, but in the case of the d-electron donor V^{II} ion the dependence on hydrogen ion concentration is canceled out by the inverse dependence in the preceding complex formation. This does not seem to be the case with Eu^{II} ion.

Registry No. Eu^{2+} , 16910-54-6; pyr, 127-17-3; lactic acid, 50-21-5.

(8) Unpublished results of the present authors.

Contribution from the Department of Chemistry, Faculty of Science, Tohoku University, Aoba, Aramaki, Sendai 980, Japan

Kinetics and Mechanisms of the Cleavage of the Chromium–Carbon Bond in (Ethylenediamine-*N,N,N',N'*-tetraacetato)(hydroxyalkyl)chromium(III) Complexes

HIROSHI OGINO,* MAKOTO SHIMURA, and NOBUYUKI TANAKA

Received April 29, 1981

Kinetic measurements of the cleavage of the Cr–C bond in (ethylenediamine-*N,N,N',N'*-tetraacetato)(hydroxyalkyl)chromium(III) complexes, $[\text{Cr}(\text{CR}_1\text{R}_2\text{OH})(\text{EDTA})]^{2-}$ ($\text{R}_1, \text{R}_2 = \text{H}$ or CH_3), to give $[\text{Cr}(\text{EDTA})(\text{H}_2\text{O})]^-$ were made at ionic strength of 1.0 (LiClO_4). The reactions obeyed the rate law $-d[\text{complex}]/dt = (k_0 + k_1[\text{H}^+])[\text{complex}]$ for the CH_2OH and $\text{C}(\text{CH}_3)_2\text{OH}$ complexes and the rate law $-d[\text{complex}]/dt = [(k_0 + k_1[\text{H}^+]) / (1 + Q[\text{H}^+])] [\text{complex}]$ for the $\text{CH}(\text{CH}_3)\text{OH}$ complex. The rate constants at 25.0 °C were $k_0 = (2.52 \pm 0.22) \times 10^{-4} \text{ s}^{-1}$ and $k_1 = 256 \pm 3 \text{ M}^{-1} \text{ s}^{-1}$ for $[\text{Cr}(\text{CH}_2\text{OH})(\text{EDTA})]^{2-}$, $k_0 = (1.35 \pm 0.11) \times 10^{-3} \text{ s}^{-1}$ and $k_1 = 73.5 \pm 4.2 \text{ M}^{-1} \text{ s}^{-1}$ for $[\text{Cr}(\text{CH}(\text{CH}_3)\text{OH})(\text{EDTA})]^{2-}$, and $k_0 = (1.38 \pm 0.03) \times 10^{-2} \text{ s}^{-1}$ and $k_1 = 176 \pm 3 \text{ M}^{-1} \text{ s}^{-1}$ for $[\text{Cr}(\text{C}(\text{CH}_3)_2\text{OH})(\text{EDTA})]^{2-}$. The activation parameters of these reactions were also determined. The value of Q was determined to be $2 \times 10^3 \text{ M}^{-1}$ at 25.0 °C. Comparison of the kinetic parameters with those of the corresponding (hydroxyalkyl)pentaaqua complexes indicates that the uncoordinated carboxylic acid group of the coordinated EDTA acts as an internal electrophile to the chromium-bound carbon atom.

Introduction

Schmidt et al. reported the preparation of (hydroxyalkyl)pentaaquachromium(III) complexes ($[\text{CrR}(\text{H}_2\text{O})_5]^{2+}$) and the kinetics of the acid hydrolyses of $[\text{CrR}(\text{H}_2\text{O})_5]^{2+}$ to $[\text{Cr}(\text{H}_2\text{O})_6]^{3+}$.¹ It was found, in the present work, that analogous reactions in the presence of ethylenediamine-*N,N,N',N'*-tetraacetate afforded (ethylenediaminetetraacetato)(hydroxyalkyl)chromium(III) complexes (hereafter abbreviated as $[\text{CrR}(\text{EDTA})]^{2-}$), in which the R ligands were CH_2OH^- , $\text{CH}(\text{CH}_3)\text{OH}^-$, and $\text{C}(\text{CH}_3)_2\text{OH}^-$. This paper describes the preparation of $[\text{CrR}(\text{EDTA})]^{2-}$ and the kinetic results of the cleavage reactions of the Cr–C bonds in these complexes. Through the comparison of the kinetic behaviors of the $[\text{CrR}(\text{EDTA})]^{2-}$ complexes with those of the corresponding $[\text{CrR}(\text{H}_2\text{O})_5]^{2+}$ complexes, a unique effect of the

EDTA ligand on the rate of the Cr–C bond cleavage will be discussed.

Experimental Section

Materials. Redistilled water was used to prepare all the solutions. The solutions of $[\text{Cr}(\text{H}_2\text{O})_6](\text{ClO}_4)_2$ were prepared by the reduction of $[\text{Cr}(\text{H}_2\text{O})_6](\text{ClO}_4)_3$ solutions with zinc amalgam. The $[\text{Cr}^{\text{II}}(\text{EDTA})(\text{H}_2\text{O})]^{2-}$ solutions were prepared by the addition of the $[\text{Cr}(\text{H}_2\text{O})_6]^{2+}$ solutions into solutions containing excess EDTA. An aqueous hydrogen peroxide solution (30%) was used without further purification and standardized against potassium permanganate solutions. The alcohols, methanol, ethanol, and 2-propanol, were purified by distillation. The solution of LiClO_4 was prepared as reported previously.² In most experiments, the solutions of $[\text{CrR}(\text{EDTA})]^{2-}$ complexes were prepared as follows. The $[\text{Cr}(\text{H}_2\text{O})_6]^{2+}$ solution was injected into a solution containing appropriate amounts of H_2O_2 , EDTA, and alcohol (methanol, ethanol, or 2-propanol) under a nitrogen or argon atmosphere. The initial concentrations of the reagents

(1) Schmidt, W.; Swinehart, J. H.; Taube, H. *J. Am. Chem. Soc.* **1971**, *93*, 1117.

(2) Ogin, H.; Tsukahara, K.; Tanaka, N. *Inorg. Chem.* **1979**, *18*, 1271.